STACK Crystal Chemistry

Kathleen I. Schaffers, Paul D. Thompson, Theodore Alekel III, James R. Cox, and Douglas A. Keszler*

Department of Chemistry and Center for Advanced Materials Research, Oregon State University, Gilbert Hall 153, Corvallis, Oregon 97331-4003

Received April 20, 1994. Revised Manuscript Received August 29, 1994[⊗]

The crystal chemistry of the STACK family of orthoborates having the nominal formula $A_6MM'(BO_3)_6$ where A = Sr, Ba, Pb, or Ln (Ln = lanthanide), and M, M′ = +2, +3, or +4 metal cation is described. Over 150 individual members of the family have been synthesized; they crystallize in the trigonal space group $R\bar{3}$ with unit-cell volumes ranging from 1143.8(1) to 1365.6(3) Å^3. In this report, the metal site preferences, disorder, and solid solubility of these phases are discussed. Interrelationships between this structure and the layered structure type of $Ba_3Sc(BO_3)_3$ are also detailed.

Introduction

Among the myriad of known solid-state inorganic structure types, there exist common examples such as rock salt, garnet, spinel, zinc blende, elpasolite, and perovskite where a common spatial arrangement is retained for a great variety of atomic constituents. For example, the compounds NaCl, MgO, MgS, CaO, CaS, TiO, and ScN all adopt the rock salt structure, and the oxides $Ca_3Al_2Si_3O_{12}$, $Y_3Al_5O_{12}$, $Gd_3Ga_5O_{12}$, and $Ca_3Te_2Zn_3O_{12}$ all crystallize in the garnet structure. We derive a sense of order from classifying materials in this way, but the efficacy of doing so certainly derives from the capacity to control physical properties by freely substituting selected atoms at specific sites while maintaining structural integrity. In fact, many of our modern technological advances can be traced to this ability.

In a recent contribution we reported the existence of an entirely new family of compounds whose members now comprise one of the larger structural classes of oxide reported to date.[1] This family, which we designate STACK,[2] is derived from the structure of the compound $Sr_3Sc(BO_3)_3$[3,4] by substitution of a variety of atoms at the Sr and Sc sites. The general formula is $A_6MM'(BO_3)_6$, where A = Sr, Ba, Pb, or selected lanthanides, M = Ca, Sr, Y, Sc, In, Bi, or selected lanthanides, and M′ = Mg, Al, Ga, Cr, Mn, Fe, Co, Rh, Zn, Sc, In, Zr, Hf, Sn, or selected lanthanides.

In developing the physical properties of these new materials, it will be necessary to grasp the structural consequences and patterns encountered with the various chemical substitutions. In this report, we discuss the crystal chemistry of this family and establish interrelationships with the layered structure type of the compound $Ba_3Sc(BO_3)_3$, which we described in the preceding report of this series.

Experimental Section

Synthesis. Powders of the Sr compounds were synthesized by using standard high-temperature solid-state methods. Stoichiometric quantities of the starting reagents (nitrates, carbonates, or oxides, typically ≥99.9%) were mixed with a 2 mol % excess of B_2O_3, ground under hexane, and heated at 923 K for 1 h to decompose the reagents and initiate the reactions. The samples were reground and heated for 6 h at 1028 K, 12 h at 1123 K, and 24 h in the range 1173−1673 K, depending on the sintering characteristics of the sample. Analysis of powder X-ray diffraction patterns obtained with a Philips automated diffractometer confirmed the formation of the desired product. Further synthesis studies on the derivatives $Sr_3Sc(BO_3)_3$ and $Sr_6YAl(BO_3)_6$ revealed that they could be synthesized by using a flash-synthesis method.[5] In this method, the reagents were ground under hexane and heated in a Pt crucible directly at 923 K for 20 min and 1023 K for 15 min to initiate the reaction. The powder was then ground and heated promptly at 1273 K for 3 h. It is likely that most of the Sr derivatives can be prepared in this manner.

In general, a different set of conditions is necessary for synthesis of crystalline Ba derivatives. The flash-synthesis method can only be used for a few compounds, and lower heating temperatures (1123−1223 K) are generally required to avoid melting the sample. Also, smaller incremental increases in temperature, 25−75 K after each grinding, and longer heating times are typically needed to produce homogeneous samples. Each heating period lasted 12−24 h but could be as long as several days. For example, the compound $Ba_6ErFe(BO_3)_6$ was prepared by grinding together stoichiometric ratios of the starting materials with 2 mol % excess B_2O_3 and heating at 898 K for 1 h, 1008 K for 19 h, 1073 K for 24 h, 1123 K for 21 h, and 1148 K for 14 h. The compound $Ba_6GdSc(BO_3)_6$, however, is readily prepared by flash heating.

Powder data for the materials were collected on an automated Philips diffractometer; peak positions were corrected by using NIST Si Standard 640b. Unit-cell parameters were refined by least-squares analysis with 11 peaks in the range $26 \leq 2\theta \leq 58°$. The *hkl* assignments of each reflection were determined by comparison to powder X-ray patterns of the parent material $Sr_3Sc(BO_3)_3$[3,4] and other selected derivatives.

To establish experimental variation in unit-cell parameters, six pairs of samples were compared to determine the variance of their cell parameters **a** and **c** and unit-cell volumes **V**. The maximum differences found (Δa, Δc, and ΔV) were used as an estimate of the maximum deviation from an average value. Reported values were found to be within ±0.1% for **a**, ±0.2% for **c**, and ±0.5% for **V**. Actual statistical deviations from the refinements with X-ray data are included in parentheses in Table 3. In each case inclusion of a larger cation should result in a larger unit cell, but this may not occur if the enlargement is less than the experimental errors associated with the

* To whom correspondence should be addressed.

⊗ Abstract published in *Advance ACS Abstracts,* October 15, 1994.

(1) Schaffers, K. I.; Alekel III, T.; Thompson, P. D.; Cox, J. R.; Keszler, D. A. *J. Am. Chem. Soc.* **1990**, *112*, 7068.

(2) The term STACK derives, in part, from the structural description; it is also an acronym from the surnames of the authors.

(3) Thompson, P. D.; Keszler, D. A. *Chem. Mater.* **1988**, *1*, 292.

(4) Thompson, P. D.; Keszler, D. A. *Chem. Mater.*, first of three papers in this issue.

(5) Schaffers, K. I.; Keszler, D. A. *Inorganic Syntheses*; Wiley: New York, in press.

0897-4756/94/2806-2014$04.50/0

Table 1. Crystal Data for STACK Borates

	$Sr_6Y_{1.07}Al_{0.93}(BO_3)_6$	$Sr_6Er_{1.40}Sc_{0.60}(BO_3)_6$	$Sr_6Ho_{0.964}Sc_{1.036}(BO_3)_6$	$Sr_6La_{0.84}Sc_{1.16}(BO_3)_6$	$Ba_6Gd_{1.28}Sc_{0.72}(BO_3)_6$
formula wt, amu	994.46	1090.79	1088.45	1102.51	1379.04
crystal system			rhombohedral		
space group			$R\bar{3}$		
a, Å	12.162(3)	12.322(1)	12.285(3)	12.388(1)	12.960(1)
c, Å	9.103(4)	9.293(2)	9.268(2)	9.294(2)	9.538(2)
V, Å^3	1166.1(8)	1221.8(3)	1211.2(5)	1235.2(2)	1387.2(3)
Z	3	3	3	3	3
D_{calc}, g cm^{-3}	4.248	4.447	4.476	4.446	4.952
$F(000)$	1362	1473	1470	1500	1785
diffractometer			Rigaku AFC6R		
radiation			Mo Kα (λ=0.71069 Å)		
data collected			+h, ±k, ±l		
no. of observations ($F_o^2 \geq 3\sigma(F_o^2)$)	568	835	693	920	1191
R	0.040	0.034	0.025	0.048	0.055
R_w	0.042	0.045	0.039	0.068	0.063

compound synthesis and cell parameter determination. Reported esd's in the cell parameter tables have their origin in the POLSQ program and reflect the uncertainty with which the least-squares fit has settled on a specific value. Actual variations in unit cell parameters up to 0.019 Å are an order of magnitude larger than esd's indicated by POLSQ. Sources of experimental error include the precision in weighing the starting reagents which can skew the stoichiometry of the product, and for some samples, deviation from the nominal composition may be expected. Also, in a few cases, poor sample crystallinity affords broad and asymmetric diffraction peaks that lead to uncertainties in selecting peak positions.

Crystal Growth. Single crystals of $Sr_6Y_{1.07}Al_{0.93}(BO_3)_6$, $Sr_6Ho_{0.964}Sc_{1.036}(BO_3)_6$, $Sr_6Er_{1.40}Sc_{0.60}(BO_3)_6$, $Sr_6La_{0.84}Sc_{1.16}(BO_3)_6$, and $Ba_6Gd_{1.28}Sc_{0.72}(BO_3)_6$ were grown by slowly cooling melts. Crystals of $Sr_6Y_{1.07}Al_{0.93}(BO_3)_6$ were seized from a melt with the following mol % composition: 61.5 SrO, 5.1 Y_2O_3, 7.9 Al_2O_3, 20.5 B_2O_3, and 5.1 Li_2O. The melt was cooled from 1273 K to 1073 K at 10 K/h and then to room temperature at 100 K/h. A crystal was removed from the matrix by dissolution of the flux in dilute HNO_3(aq). Crystals of $Sr_6HoSc(BO_3)_6$ were grown by melting a stoichiometric sample in a Pt crucible at 1773 K followed by cooling at 4 K/h to 1273 K and 40 K/h to room temperature. A crystal of $Sr_6Er_{1.40}Sc_{0.60}(BO_3)_6$ was isolated from a melt corresponding to the stoichiometric proportions of $Sr_6ErSc(BO_3)_6$. The heating and cooling programs were the same as those applied to the Ho crystals. Crystals of $Sr_6La_{0.84}Sc_{1.16}(BO_3)_6$ were obtained from a melt of 70 mol % $Sr_6LaSc(BO_3)_6$: 30 mol % CaF_2 that was cooled from 1648 to 1348 K at 15 K/h followed by cooling to room temperature at 130 K/h. Single crystals of $Ba_6Gd_{1.28}Sc_{0.72}(BO_3)_6$ were grown by melting the stoichiometric material $Ba_6GdSc(BO_3)_6$ in a Pt crucible at 1573 K and then cooling to 1373 K at 5 K/h and at 40 K/h to room temperature.

Single-Crystal Work. Relevant crystal data for each of the structures are presented in Table 1.

$Sr_6Y_{1.07}Al_{0.93}(BO_3)_6$. A 0.2 × 0.2 × 0.2 mm crystal was selected for analysis. The data were collected on a Rigaku AFC6 rotating anode diffractometer equipped with a graphite monochromator set for Mo Kα radiation. 2381 reflections were measured by using $\omega-2\theta$ scans in covering the range of indexes $0 \leq h \leq 17$, $-17 \leq k \leq 17$, and $-12 \leq l \leq 12$ to $2\theta_{max} = 60°$. From these data, 764 unique reflections with $F_o^2 \geq 3\sigma(F_o^2)$ were available for structure determination and refinement. Three standard reflections measured after each block of 200 data exhibited excursions of less than 2.5%. A Digital μVAX-II computer, together with programs from the TEXSAN crystallographic software package,[6] were used to solve the structure. The heavy atoms Sr and Y were located by using the direct methods program SHELXS,[7] and the positions of the other atoms were determined from analysis of difference electron density maps. After several cycles of least-squares refinement, the isotropic displacement coefficient at the Al site had refined to a negative value, indicating the presence of additional electron density. The multiplicity of the site was subsequently refined to a value greater than unity. It was then modeled with two disordered atoms (Y and Al) where the population was fixed at unity and the x, y, z, and B parameters of the Y atom were constrained to those of the Al atom. Refinement of the multiplicity indicated that 7.3% of the Al sites were occupied by Y atoms to give the more exacting formula $Sr_6Y(Al_{0.927}Y_{0.073})(BO_3)_6$. The data were corrected for absorption with the program DIFABS[8] and subsequently averaged ($R_{int} = 0.108$). Anisotropic displacement coefficients were applied to the Sr, Y, B, and O sites in refinement to the final residuals $R = 0.040$ and $R_w = 0.042$. The largest peak in the final difference electron density map corresponds to 0.96% of an Y atom.

$Sr_6Ho_{0.964}Sc_{1.036}(BO_3)_6$. A single crystal of approximate dimensions 0.15 × 0.17 × 0.20 mm was selected for structure analysis on the same diffractometer. From 2456 reflections measured to $2\theta_{max} = 60°$ over the range of indexes $0 \leq h \leq 17$, $-17 \leq k \leq 17$, and $-13 \leq l \leq 13$, 693 unique reflections with $F_o^2 \geq 3\sigma(F_o^2)$ were obtained. Three standards measured after every 200 reflections deviated on average by less than 1.5%. Each of the atoms was positioned by comparison to the isostructural compound $Sr_3Sc(BO_3)_3$.[3,4] After several cycles of least-squares refinement, examination of the isotropic displacement coefficients indicated a disorder over the Ho1 and Sc1 sites. They were then modeled with two atoms at each position with the occupancy of each site constrained to unity. The B values of atoms Sc2 and Ho2 were constrained to those of atoms Ho1 and Sc1, respectively. The data were corrected for absorption with the program DIFABS and subsequently averaged ($R_{int} = 0.045$). Least-squares refinement with anisotropic displacement coefficients on the Sr, B, and O atoms and an extinction parameter = $0.19(3) \times 10^{-6}$ afforded the final residuals $R = 0.027$ and $R_w = 0.041$. The largest peak in the final difference electron density map corresponds to 0.27% of a Ho atom. A descriptive formula representing the final result is $Sr_6(Ho_{0.892(5)}Sc_{0.108})(Sc_{0.928(4)}Ho_{0.072})(BO_3)_6$.

$Sr_6Er_{1.40}Sc_{0.60}(BO_3)_6$. A crystal of approximate dimensions 0.20 × 0.20 × 0.25 mm was mounted on the Rigaku diffractometer for structure analysis. Cell constants were obtained from least-squares refinement of the setting angles of 15 reflections in the range $36 < 2\theta < 42°$. From 2135 reflections of the type h, $\pm k$, $\pm l$ measured to $2\theta_{max} = 65°$, 979 unique reflections were obtained. The positions of the heavy atoms Sr, Er, and Sc were taken from the solution of the Ho analog. The positions of the B and O atoms were subsequently determined from analyses of difference electron density maps. The actual occupancies of the Er and Sc sites were determined in a manner similar to that used for the Ho derivative. The data were corrected for absorption and averaged ($R_{int} = 0.067$). The Er and Sc sites were subsequently refined with isotropic displacement coefficients, while the remaining atoms were refined with anisotropic coefficients. Final refinement on F_o with data having $F_o^2 \geq 3\sigma(F_o^2)$ and a secondary extinction

(6) TEXSAN: Single Crystal Structure Analysis Software, Version 5.0, 1989, Molecular Structure Corporation, The Woodlands, TX 77381.

(7) Sheldrick, G. M. *Crystallographic Computing 3*; Oxford University Press: Oxford, 1985.

(8) Walker, N.; Stuart, D. *Acta Crystallogr., Sect. A* **1983**, *39*, 158.

Table 2. Positional Parameters for STACK Borates

A		$Sr_6Y_{1.07}Al_{0.93}(BO_3)_6$[a]	$Sr_6Er_{1.40}Sc_{0.60}(BO_3)_6$[b]	$Sr_6Ho_{0.964}Sc_{1.036}(BO_3)_6$[c]	$Sr_6La_{0.84}Sc_{1.16}(BO_3)_6$[d]	$Ba_6Gd_{1.28}Sc_{0.72}(BO_3)_6$[e]
A	x	0.57169(4)	0.57542(5)	0.57425(5)	0.57741(5)	0.57506(3)
	y	0.04230(4)	0.04144(5)	0.04197(5)	0.04338(5)	0.04058(3)
	z	0.69465(6)	0.68987(6)	0.69082(5)	0.69168(6)	0.69372(4)
	B_{eq}	0.70(2)	0.60(2)	0.55(2)	0.87(2)	1.21(2)
M	x	0	0	0	0	0
	y	0	0	0	0	0
	z	0	0	0	0	0
	B_{eq}	0.50(2)	0.35(2)	0.31(2)	0.76(3)	1.05(2)
M′	x	0	0	0	0	0
	y	0	0	0	0	0
	z	1/2	1/2	1/2	1/2	1/2
	B_{eq}	0.38(5)	0.46(2)	0.20(5)	0.89(6)	2.80(8)
B	x	0.1906(5)	0.1982(6)	0.1974(5)	0.2014(7)	0.1936(8)
	y	0.1354(5)	0.1427(5)	0.1407(5)	0.1433(7)	0.1378(7)
	z	0.7569(8)	0.7614(7)	0.7597(6)	0.7572(8)	0.7558(9)
	B_{eq}	0.7(2)	0.6(2)	0.5(2)	0.9(2)	1.6(2)
O1	x	0.1717(3)	0.1686(4)	0.1683(4)	0.1555(4)	0.1691(6)
	y	0.6327(3)	0.6254(4)	0.6276(4)	0.6228(5)	0.6257(6)
	z	0.8175(5)	0.8149(5)	0.8154(4)	0.8255(6)	0.8217(8)
	B_{eq}	1.1(1)	0.9(1)	0.8(1)	1.2(1)	2.6(2)
O2	x	0.6234(3)	0.6150(4)	0.6170(4)	0.6217(5)	0.6207(5)
	y	0.1802(3)	0.1643(4)	0.1687(4)	0.1669(5)	0.1734(5)
	z	0.9443(4)	0.9501(5)	0.9483(4)	0.9465(5)	0.9509(6)
	B_{eq}	0.9(1)	1.0(1)	0.8(1)	1.6(2)	1.9(2)
O3	x	0.5954(3)	0.5937(4)	0.5949(4)	0.5911(5)	0.5879(5)
	y	−0.0762(3)	−0.0712(4)	−0.0731(4)	−0.0720(5)	−0.0825(5)
	z	0.4724(5)	0.4763(5)	0.4756(4)	0.4766(6)	0.4726(7)
	B_{eq}	1.0(1)	1.1(1)	0.9(1)	1.6(2)	2.1(2)

[a] A = Sr; M = Y; M′ = Al(0.93), Y(0.07). [b] A = Sr; M = Er(0.915), Sc(0.085); M′ = Er(0.488), Sc(0.512). [c] A = Sr; M = Ho(0.892), Sc(0.108); M′ = Sc(0.928), Ho(0.072). [d] A = Sr(5.16), La(0.84); M = Sr(.84), Sc(0.16); M′ = Sc. [e] A = Ba; M = Gd(0.92), Sc(0.08); M′ = Sc(0.66), Gd(0.34).

coefficient = $0.25(2) \times 10^{-6}$ afforded the final residuals R = 0.034 and R_w = 0.045. The largest peak in the final difference electron density map corresponds to 1.8% of a Sr atom. The formula that indicates the occupancies of the disordered sites is $Sr_6(Er_{0.915(5)}Sc_{0.085})(Er_{0.488(5)}Sc_{0.512})(BO_3)_6$.

$Sr_6La_{0.84}Sc_{1.16}(BO_3)_6$. A crystal of approximate size 0.2 × 0.2 × 0.3 mm was mounted for structure analysis. Cell constants were obtained from least-squares refinement with the setting angles of 17 centered reflections in the range 30.5 ≤ 2θ ≤ 36°. Three standard reflections measured throughout the data collection exhibited no significant variations. From 3741 reflections measured over the range of indexes $-19 \le h \le 19$, $0 \le k \le 19$, and $-15 \le l \le 15$ to $2\theta_{max} = 70°$, 1205 unique reflections were obtained. The atoms on special positions were placed by analogy to the previous structures, and the remaining atoms were found by interpretation of difference electron density maps. Approximate site occupancies were determined by refining multiplicities with Sr atoms in the general-position sites and the special position 0, 0, 1/2. These occupancies were subsequently modeled with partial substitution of La on the general position and Sc on the special position. The refinement was then constrained to give a total unit occupancy for the special position and an appropriate La concentration on the general position to maintain charge neutrality. Following refinement of the model with isotropic displacement factors, the data were corrected for absorption and merged (R_{int} = 0.073). Final refinement with anisotropic displacement coefficients on the Sc1, B, and O atoms and an extinction correction = $0.8(1) \times 10^{-6}$ afforded the residuals R = 0.048 and R_w = 0.068. The largest peak in the final difference electron density map corresponds to 4% of a Sc atom. The final results afford the descriptive formula $(Sr_{5.16}La_{0.84})(Sr_{0.84(2)}Sc_{0.16})Sc(BO_3)_6$.

$Ba_6Gd_{1.28}Sc_{0.72}(BO_3)_6$. A single crystal of approximate dimensions 0.1 × 0.1 × 0.15 mm was selected for structure determination. A total of 1176 unique reflections having $F_o^2 \ge 3\sigma(F_o^2)$ were obtained by using the ω–2θ scan technique to collect 4197 reflections in the range 2 ≤ 2θ ≤ 80°. Three standards measured throughout the data collection exhibited an average deviation of 0.23%. The position of the Ba atom was determined from the results of the direct methods program SHELXS, and the Gd and Sc atoms were located by analogy to the structure described above. The remaining atoms were placed following examination of difference electron density maps. The magnitude of the temperature factors after least-squares refinement indicated disorder at the Gd and Sc sites. Refinement of the multiplicities gave 13% Sc on the Gd site and 41% Gd on the Sc site so that the formula is $Ba_6(Gd_{0.869(3)}Sc_{0.131})(Sc_{0.589},Gd_{0.411(4)})(BO_3)_6$. The data were corrected for absorption with the program DIFABS and averaged (R_{int} = 0.080). The Ba, B, and O atoms were refined with anisotropic displacement coefficients, and the remaining atoms were refined with isotropic parameters. The larger resulting displacement coefficients for this structure in comparison with those of the others reported here likely results from the higher degree of disorder and the larger size differential (Gd^{3+} vs Sc^{3+}) for the atoms on the M and M′ sites. The converged refinement affords the final residuals R = 0.055 and R_w = 0.063. The largest peak in the difference electron density map corresponds to 3.5% of a Gd atom. Positional parameters and equivalent isotropic displacement coefficients for each of the structures are summarized in Table 2.

Results and Discussion

A listing of the STACK compounds that we have prepared along with their unit-cell parameters is given in Table 3. The unit-cell volumes range from 1143.8(1) Å^3 for the compound $Sr_6ScAl(BO_3)_6$ to 1414.0(2) Å^3 for the derivative $Ba_6SrZr(BO_3)_6$. The precision attained in the refinement of the parameters is an indication of the high crystallinity of most of the samples. They are, in fact, hard, dense, and stable ceramic materials, much like the members of other oxide families such as spinel and perovskite. Melting points of the more stable derivatives extend to approximately 1723 K.

The nominal formula $A_6MM'(BO_3)_6$ results from structural considerations of the parent compound $Sr_3Sc(BO_3)_3 \equiv Sr_6ScSc'(BO_3)_6$. As reported in the first paper of this series, the structure is a high-symmetry trigonal type forming in a rhombohedral cell. It contains two types of Sc-centered O octahedra that alternately *stack* between planar triangular BO_3 groups to form chains

Table 3. Cell Parameters for Compounds of the STACK Family

compound	a (Å)	c (Å)	V (Å^3)	compound	a (Å)	c (Å)	V (Å^3)
$Sr_6ScAl(BO_3)_6$	12.082(1)	9.047(1)	1143.8(1)	$Sr_6BiFe(BO_3)_6$	12.310(2)	9.215(2)	1209.4(3)
$Sr_6ScCr(BO_3)_6$	12.104(1)	9.095(2)	1154.0(2)	$Sr_6NdGa(BO_3)_6$	12.330(1)	9.189(1)	1209.9(2)
$Sr_6LuAl(BO_3)_6$	12.141(1)	9.071(2)	1158.1(2)	$LaSr_5ScCo(BO_3)_6$	12.290(1)	9.251(2)	1210.1(2)
$Sr_6YbAl(BO_3)_6$	12.147(1)	9.077(1)	1159.9(2)	$Sr_6DySc(BO_3)_6$	12.288(1)	9.257(1)	1210.6(1)
$Sr_6InCr(BO_3)_6$	12.136(2)	9.116(3)	1162.7(4)	$LaSr_5ScNi(BO_3)_6$	12.295(1)	9.250(1)	1210.9(1)
$Sr_6TmAl(BO_3)_6$	12.160(1)	9.092(1)	1164.2(1)	$Sr_5BaHoFe(BO_3)_6$	12.316(2)	9.219(2)	1211.0(3)
$Sr_6InMn(BO_3)_6$	12.138(2)	9.136(2)	1165.8(3)	$Sr_6YSc(BO_3)_6$	12.284(1)	9.268(2)	1211.2(4)
$Sr_6ErAl(BO_3)_6$	12.171(1)	9.097(2)	1166.9(3)	$Sr_6HoSc(BO_3)_6$	12.285(3)	9.268(2)	1211.2(5)
$Sr_6ScGa(BO_3)_6$	12.143(1)	9.146(1)	1167.8(2)	$Sr_6GdMn(BO_3)_6$	12.330(4)	9.206(4)	1212.0(7)
$Sr_6HoAl(BO_3)_6$	12.182(1)	9.095(2)	1169.0(2)	$LaSr_5MgAl(BO_3)_6$	12.314(1)	9.232(1)	1212.3(2)
$Sr_6YbGa(BO_3)_6$	12.174(1)	9.120(2)	1170.4(2)	$Sr_6TbIn(BO_3)_6$	12.329(1)	9.219(1)	1213.5(3)
$Sr_6ScSc(BO_3)_6$	12.135(1)	9.184(1)	1171.3(3)	$PrSr_5ScZn(BO_3)_6$	12.307(1)	9.252(1)	1213.6(1)
$Sr_6YAl(BO_3)_6$	12.190(2)	9.109(5)	1172.3(5)	$Sr_6LaG(BO_3)_6$	12.339(1)	9.209(1)	1214.3(1)
$Sr_6LuGa(BO_3)_6$	12.187(2)	9.130(3)	1174.5(4)	$Sr_6TbSc(BO_3)_6$	12.306(2)	9.263(3)	1214.9(4)
$Sr_6ErGa(BO_3)_6$	12.190(1)	9.128(1)	1174.6(2)	$La_2Sr_4SrZn(BO_3)_6$	12.319(2)	9.264(2)	1217.4(3)
$SmSr_5YNi(BO_3)_6$	12.175(2)	9.159(3)	1175.9(3)	$La_2Sr_4SrMg(BO_3)_6$	12.318(1)	9.254(2)	1216.1(2)
$Sr_6DyAl(BO_3)_6$	12.218(1)	9.111(1)	1177.9(1)	$Sr_6EuSc(BO_3)_6$	12.327(1)	9.262(1)	1219.0(2)
$Sr_6TbAl(BO_3)_6$	12.218(1)	9.115(1)	1178.3(1)	$LaSr_5ScZn(BO_3)_6$	12.327(1)	9.266(2)	1219.3(2)
$Pb_2Sr_4ScSc(BO_3)_6$	12.171(1)	9.186(1)	1178.4(2)	$Sr_6EuIn(BO_3)_6$	12.361(1)	9.234(1)	1221.9(2)
$PrSr_5YNi(BO_3)_6$	12.182(2)	9.170(2)	1178.4(3)	$Sr_6CaSn(BO_3)_6$	12.381(1)	9.206(1)	1222.0(1)
$NdSr_5YMg(BO_3)_6$	12.185(1)	9.180(2)	1180.4(2)	$Sr_6SmSc(BO_3)_6$	12.350(1)	9.276(2)	1225.2(2)
$Sr_6GdAl(BO_3)_6$	12.230(1)	9.114(2)	1180.6(3)	$La_2Sr_4CdCd(BO_3)_6$	12.364(1)	9.273(2)	1227.6(2)
$Sr_6YCr(BO_3)_6$	12.213(1)	9.146(1)	1181.5(2)	$LaSr_5CaSc(BO_3)_6$	12.378(1)	9.273(2)	1230.4(3)
$Sr_6InSc(BO_3)_6$	12.184(2)	9.190(2)	1181.5(3)	$Sr_6NdSc(BO_3)_6$	12.373(1)	9.286(1)	1231.0(2)
$Sr_6YRh(BO_3)_6$	12.228(2)	9.126(2)	1181.7(3)	$Sr_6GdSc(BO_3)_6$	12.395(3)	9.262(4)	1232.3(6)
$Sr_6HoGa(BO_3)_6$	12.220(1)	9.150(1)	1183.3(2)	$Sr_6PrSc(BO_3)_6$	12.384(1)	9.293(1)	1234.2(1)
$NdSr_5YNi(BO_3)_6$	12.208(2)	9.169(2)	1183.4(3)	$Sr_6CdSn(BO_3)_6$	12.434(2)	9.236(2)	1236.5(3)
$LaSr_5ErNi(BO_3)_6$	12.199(1)	9.184(1)	1183.6(2)	$LaSr_5SrSc(BO_3)_6$	12.398(1)	9.302(1)	1238.1(2)
$SmSr_5YZn(BO_3)_6$	12.205(1)	9.177(2)	1183.9(3)	$Sr_6LuLu(BO_3)_6$	12.433(1)	9.262(2)	1239.9(3)
$LaSr_5YNi(BO_3)_6$	12.202(1)	9.187(1)	1184.6(1)	$Sr_6SrSn(BO_3)_6$	12.464(1)	9.241(1)	1243.2(1)
$SmSr_5YMg(BO_3)_6$	12.213(1)	9.171(2)	1184.6(3)	$Sr_6ErEr(BO_3)_6$	12.478(1)	9.240(1)	1246.0(2)
$Sr_6YGa(BO_3)_6$	12.223(2)	9.159(2)	1185.0(3)	$LaSr_5SrCd(BO_3)_6$	12.425(1)	9.324(1)	1246.5(1)
$LaSr_5HoNi(BO_3)_6$	12.209(1)	9.185(1)	1185.7(1)	$Sr_6CdHf(BO_3)_6$	12.412(1)	9.346(2)	1246.8(3)
$NdSr_5HoCo(BO_3)_6$	12.218(1)	9.179(1)	1186.7(1)	$Sr_6YY(BO_3)_6$	12.503(2)	9.248(2)	1252.1(4)
$Sr_6EuAl(BO_3)_6$	12.254(1)	9.126(2)	1186.7(2)	$Sr_6DyDy(BO_3)_6$	12.487(3)	9.234(3)	1246.9(4)
$Sr_6SmAl(BO_3)_6$	12.258(1)	9.126(1)	1187.5(2)	$Sr_6HoHo(BO_3)_6$	12.509(1)	9.254(1)	1254.0(2)
$Sr_6HoFe(BO_3)_6$	12.223(1)	9.188(1)	1188.8(2)	$Sr_6TbTb(BO_3)_6$	12.521(1)	9.247(1)	1255.4(2)
$PrSr_5YZn(BO_3)_6$	12.217(2)	9.197(3)	1188.8(4)	$Sr_6GdGd(BO_3)_6$	12.534(2)	9.251(3)	1258.7(4)
$PrSr_5YMg(BO_3)_6$	12.227(1)	9.188(2)	1189.5(2)	$Sr_6CaZr(BO_3)_6$	12.453(1)	9.367(1)	1258.0(2)
$LaSr_5CaAl(BO_3)_6$	12.258(2)	9.141(2)	1189.5(3)	$Sr_6CaHf(BO_3)_6$	12.460(2)	9.358(3)	1258.3(4)
$Sr_6YFe(BO_3)_6$	12.235(2)	9.192(2)	1191.7(3)	$Sr_6CdZr(BO_3)_6$	12.469(2)	9.371(2)	1261.7(4)
$LaSr_5YCo(BO_3)_6$	12.236(1)	9.199(1)	1192.8(2)	$Sr_6SrHf(BO_3)_6$	12.493(1)	9.373(1)	1266.9(1)
$Sr_6LuSc(BO_3)_6$	12.225(7)	9.217(1)	1192.9(2)	$Sr_6SrZr(BO_3)_6$	12.512(1)	9.392(1)	1273.5(1)
$NdSr_5ErCo(BO_3)_6$	12.251(1)	9.180(2)	1193.1(2)	$LaSr_5SrY(BO_3)_6$	12.578(3)	9.317(3)	1276.5(5)
$Sr_6EuGa(BO_3)_6$	12.261(1)	9.166(1)	1193.3(1)	$Sr_3Ba_3HoFe(BO_3)_6$	12.663(3)	9.301(3)	1291.6(5)
$LaSr_5YZn(BO_3)_6$	12.235(1)	9.206(1)	1193.5(1)	$Ba_6InIn(BO_3)_6$	12.769(1)	9.737(1)	1323.4(2)
$Sr_6BiAl(BO_3)_6$	12.279(1)	9.142(2)	1193.7(2)	$Ba_6YFe(BO_3)_6$	12.797(1)	9.372(2)	1329.1(2)
$LaSr_5HoCo(BO_3)_6$	12.241(1)	9.204(1)	1194.3(2)	$Ba_6ErFe(BO_3)_6$	12.796(0)	9.364(0)	1327.9(1)
$LaSr_5TbNi(BO_3)_6$	12.243(1)	9.202(1)	1194.5(2)	$Ba_6HoFe(BO_3)_6$	12.796(2)	9.383(4)	1330.4(6)
$LaSr_5YMg(BO_3)_6$	12.237(2)	9.215(3)	1194.9(4)	$Ba_6LuIn(BO_3)_6$	12.809(2)	9.395(2)	1334.8(3)
$Sr_6DyGa(BO_3)_6$	12.274(2)	9.158(2)	1194.9(4)	$Ba_6DyFe(BO_3)_6$	12.815(1)	9.387(2)	1335.1(3)
$LaSr_5HoMg(BO_3)_6$	12.250(1)	9.200(2)	1195.6(3)	$Ba_6TbFe(BO_3)_6$	12.818(1)	9.398(1)	1337.2(1)
$NdSr_5YZn(BO_3)_6$	12.257(2)	9.199(3)	1196.8(3)	$Ba_6YbIn(BO_3)_6$	12.818(1)	9.414(1)	1339.6(1)
$NdSr_5ScMg(BO_3)_6$	12.257(2)	9.210(3)	1198.2(4)	$Ba_6GdFe(BO_3)_6$	12.830(1)	9.408(1)	1341.1(1)
$LaSr_5EuNi(BO_3)_6$	12.254(1)	9.214(1)	1198.3(1)	$Ba_6TmIn(BO_3)_6$	12.821(1)	9.421(3)	1341.2(5)
$PrSr_5ScMg(BO_3)_6$	12.251(1)	9.222(1)	1198.7(2)	$Ba36EuFe(BO_3)_6$	12.835(1)	9.415(1)	1343.2(2)
$Sr_6InIn(BO_3)_6$	12.249(2)	9.228(3)	1199.0(5)	$Ba_6SmFe(BO_3)_6$	12.835(1)	9.416(2)	1343.4(2)
$NdSr_5TbCo(BO_3)_6$	12.269(1)	9.199(2)	1199.2(2)	$Ba_6ErIn(BO_3)_6$	12.842(1)	9.427(1)	1346.5(2)
$NdSr_5ScCo(BO_3)_6$	12.257(1)	9.220(2)	1199.6(2)	$Ba_6DySc(BO_3)_6$	12.832(1)	9.446(1)	1347.0(2)
$LaSr_5HoZn(BO_3)_6$	12.265(2)	9.209(3)	1199.6(5)	$Ba_6HoIn(BO_3)_6$	12.853(1)	9.424(2)	1348.4(3)
$NdSr_5ErZn(BO_3)_6$	12.272(1)	9.198(1)	1199.7(2)	$Ba_6YIn(BO_3)_6$	12.849(1)	9.433(2)	1348.7(2)
$Sr_6YbSc(BO_3)_6$	12.242(3)	9.246(4)	1200.0(6)	$Ba_6DyIn(BO_3)_6$	12.852(2)	9.451(2)	1352.1(4)
$Nd_2Sr_4SrMg(BO_3)_6$	12.268(1)	9.212(1)	1200.5(2)	$Ba_6TbIn(BO_3)_6$	12.851(1)	9.456(2)	1352.6(3)
$Sr_6SmGa(BO_3)_6$	12.297(1)	9.170(2)	1200.9(2)	$Ba_6TbSc(BO_3)_6$	12.849(1)	9.462(1)	1352.8(2)
$La_2Sr_4CaZn(BO_3)_6$	12.259(1)	9.233(1)	1201.7(1)	$Ba_6GdIn(BO_3)_6$	12.865(2)	9.459(3)	1355.9(4)
$NdSr_5EuZn(BO_3)_6$	12.273(1)	9.212(1)	1201.7(2)	$Ba_6SmIn(BO_3)_6$	12.878(2)	9.462(3)	1359.1(4)
$Sr_6GdFe(BO_3)_6$	12.274(1)	9.212(3)	1201.9(3)	$Ba_6EuIn(BO_3)_6$	12.886(1)	9.475(1)	1362.5(1)
$Sr_6ErSc(BO_3)_6$	12.258(1)	9.236(1)	1202.0(2)	$Ba_6GdSc(BO_3)_6$	12.880(1)	9.485(2)	1362.7(3)
$LaSr_5TbMg(BO_3)_6$	12.273(1)	9.216(2)	1202.1(2)	$Ba_6SmSc(BO_3)_6$	12.887(1)	9.491(1)	1365.0(2)
$LaSr_5TbZn(BO_3)_6$	12.273(1)	9.221(2)	1203.0(3)	$Ba_6EuSc(BO_3)_6$	12.888(1)	9.493(1)	1365.6(3)
$LaSr_5ScMg(BO_3)_6$	12.273(1)	9.229(1)	1203.9(1)	$Ba_6NdIn(BO_3)_6$	12.903(1)	9.491(2)	1368.4(3)
$Pr_2Sr_4SrMg(BO_3)_6$	12.279(1)	9.223(2)	1204.4(2)	$Ba_6PrIn(BO_3)_6$	12.918(1)	9.504(1)	1373.5(2)
$Sr_6TbGa(BO_3)_6$	12.324(1)	9.167(2)	1205.8(3)	$Ba_6NdSc(BO_3)_6$	12.950(1)	9.530(1)	1384.2(1)
$Sr_6PrGa(BO_3)_6$	12.315(1)	9.190(1)	1207.0(2)	$Ba_6PrSc(BO_3)_6$	12.946(1)	9.540(3)	1384.8(3)
$Sr_6TmSc(BO_3)_6$	12.271(2)	9.256(3)	1207.0(4)	$Ba_6LaIn(BO_3)_6$	12.965(1)	9.548(1)	1389.8(2)
$Sr_6GdGa(BO_3)_6$	12.333(1)	9.165(2)	1207.2(2)	$Ba_6LaSc(BO_3)_6$	12.981(1)	9.557(1)	1394.7(2)
$NdSr_5ScZn(BO_3)_6$	12.289(1)	9.245(1)	1209.0(1)	$Ba_6SrZr(BO_3)_6$	13.035(1)	9.609(2)	1414.0(2)
$Sr_6YMn(BO_3)_6$	12.320(2)	9.198(3)	1209.0(4)				

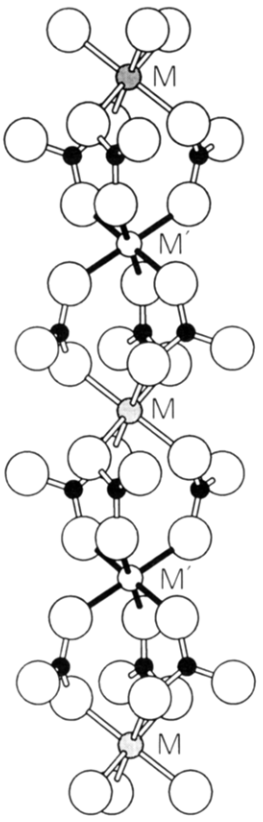

Figure 1. Chain of alternately stacked metal-centered octahedra (MO_6 and $M'O_6$) linked by BO_3 groups.

(Figure 1) that extend along the trigonal axis. The three-dimensional structure (Figure 2) results from linkage of these chains through the 9-coordinate Sr atoms. It is the specific linkages between the Sc- and Sr-centered sites that afford the nonequivalence of the octahedra. One octahedron is larger and trigonally elongated and shares only vertexes with the 9-fold site, while the other is trigonally compressed and shares its triangular faces with the 9-fold site. In the formula $A_6MM'(BO_3)_6$, A then represents an atom on the 9-coordinate site, M is an atom on the larger octahedral site, and M′ is an atom on the smaller octahedral site. For example, the formula $Sr_6YSc(BO_3)_6$ contains A = Sr, M = Y, and M′ = Sc.

We describe below in more detail the microscopic characteristics of these materials. In particular, we examine the distribution of cations among the A, M, and M′ sites, establish regions of stability within various subclasses, and illustrate the types of chemical substitutions that will allow incorporation of ~50% of the elements from the periodic table. The crystal-chemical results are certainly not exhaustive at the present time, but we can proceed in identifying important properties and trends in the family.

One subclass of the family contains the elements A = Sr and M and M′ atoms of the same type (M = M′ = Sc, In, Lu, Er, Y, Dy, Ho, Tb, and Gd), which leads to the formula $Sr_3M(BO_3)_3$. The derivative $Sr_3Sc(BO_3)_3$ ($r(Sc^{3+}) = 0.885$ Å)[9] contains the smallest equivalent M and M′ atoms while the derivative $Sr_3Gd(BO_3)_3$ ($r(Gd^{3+}) = 1.078$ Å) contains the largest. By interpolation, the structure should exist for all +3 cations of intermediate size. Hypothetical compounds such as "$Sr_3Al(BO_3)_3$" and "$Sr_3Cr(BO_3)_3$" do not exist because the +3 ions

(9) Shannon, R. D. *Acta Crystallogr., Sect. A* **1976**, *32*, 751.

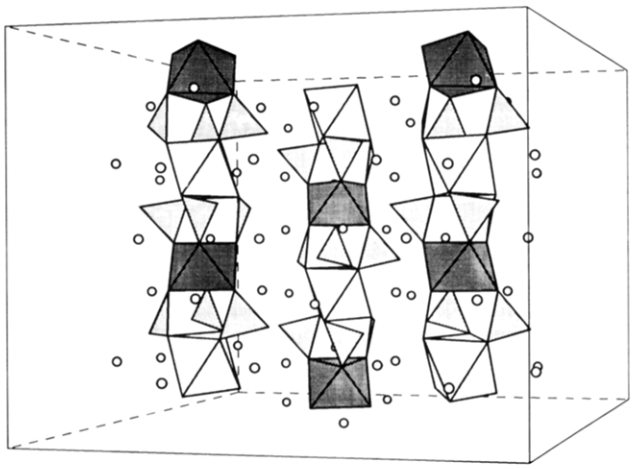

Figure 2. Sketch of the three-dimensional structure of STACK viewed orthoganol to the trigonal axis; the one-dimensional chains (Figure 1) are linked by A atoms (small open circles).

($r(Al^{3+}) = 0.675$ Å and $r(Cr^{3+}) = 0.755$ Å) are apparently too small to support the large M site. (We note that no attempts have been made to employ reducing synthesis conditions for the production of Ti^{3+} and V^{3+} derivatives.) In a similar manner, the derivative $Sr_3Eu(BO_3)_3$ does not exist because the Eu^{3+} ion is likely too large to fully occupy the small M′ site.

A larger subclass contains A = Sr and two different ions M ≠ M′ having formal charges of +3; examples include $Sr_6ScAl(BO_3)_6$, $Sr_6YFe(BO_3)_6$, and $Sr_6TbIn(BO_3)_6$. Compounds form with M and M′ cations ranging from the small Al^{3+} ion to the large lanthanide La^{3+} ($r = 1.172$ Å). To establish the approximate limits of the structure field within this subclass, we will first examine the distribution of cations over the A, M, and M′ sites. The Sc derivatives $Sr_6M''Sc(BO_3)_6$ are convenient for this purpose because the atom M″ may be any of those falling in the size range between Al^{3+} and La^{3+}, i.e., there is no immediately apparent size constraint on the existence of these phases.

To probe the characteristics of Al substitution, we examined the solid solution series $Sr_6Sc_{2-x}Al_x(BO_3)_6$ over the range $0 < x < 2$; results from powder X-ray diffraction measurements are summarized in Figure 3. As seen from the steady decrease in unit-cell volume for $x = 0$ to ~1, a complete solid solubility exists in this range. For $x > 1$, the volume remains constant, and additional phases are observed in the powder patterns. We infer from this result that the Al atom has a preference for the smaller M′ site. This supposition is consistent with the nonexistence of the phase "$Sr_3Al(BO_3)_3$."

For comparison, the results of a solid-solubility study of the series $Sr_6Y_{2-x}Al_x(BO_3)_6$ are also summarized in Figure 3. The behavior here differs markedly from the Sc series. Because of the size disparity of the Y and Al atoms, solubility exists only in the range $0 < x < \sim 0.2$. In the range $0.2 < x < 1$ simple equilibrium mixtures of the two end members, $x \approx 0.2$ and $x \approx 1$, were found to exist. Again, these results are consistent with a preference of Al atoms for the smaller M′ site, a conclusion that is verified by the single-crystal structure analysis of the compound $Sr_6Y_{1.07}Al_{0.93}(BO_3)_6$. Here, the refinement (cf. Table 2) clearly reveals principal occupation of the M′ site by the Al atom. We have carefully examined the stoichiometry of this phase by determin-

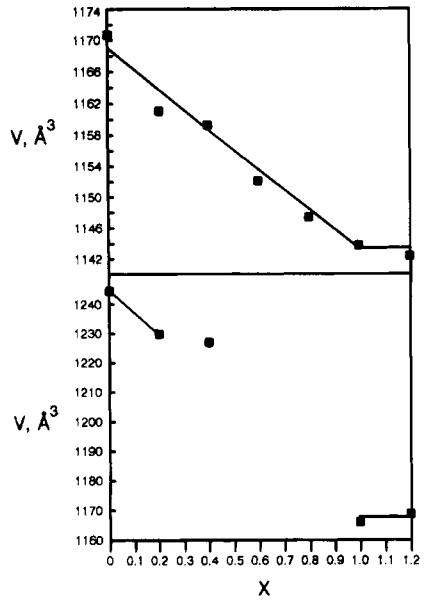

Figure 3. Cell volumes for the series $Sr_6Sc_{2-x}Al_x(BO_3)_6$ (top) and $Sr_6Y_{2-x}Al_x(BO_3)_6$ (bottom) for $0 \leq x \leq 1.2$.

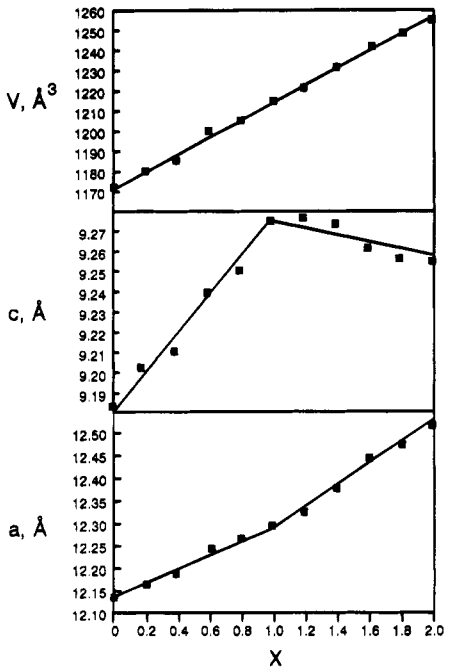

Figure 4. Cell parameters for the series $Sr_6Ho_xSc_{2-x}(BO_3)_6$ for $0 \leq x \leq 2.0$.

ing the unit-cell parameters for powder samples of $Sr_6Y_{1+x}Al_{1-x}(BO_3)_6$ with $-0.1 < x < 0.1$, and we have found no statistical variation in axial lengths or unit-cell volumes. Additionally, in the stoichiometric samples of $Sr_6YAl(BO_3)_6$, weak diffraction peaks attributable to $Sr_3(BO_3)_2$ are observed. Hence, at this stoichiometry, a very limited solubility exists, indicating that the observed composition may be a line phase.

An example of substituting a larger atom for Sc is given by the solid-solution series $Sr_6Ho_xSc_{2-x}(BO_3)_6$ ($0 < x < 2$). As seen in Figure 4, powder X-ray diffraction results reveal a steadily increasing cell volume with increasing content of the larger Ho atom and a complete solid solution over the entire range of x. The materials crystallize in a rhombohedral cell characterized by two parameters a and c. The c axis is coincident with the trigonal rotation element and the extension of the chains depicted in Figure 1. The change in the c parameter with variation in x exhibits a peculiar behavior. The parameter increases with Ho content up to $x \approx 1$, but beyond this value the parameter *decreases* even though the *larger* Ho atom is being substituted into the structure. Of course, the volume still increases in this regime because of the more steeply increasing a parameter. Our interpretation of these results is that in the region $0 < x \leq 1$ the Ho atoms exhibit a preference for the larger octahedral M site. Beyond $x \approx 1$, the Ho atoms begin to occupy the smaller octahedral M′ site. The c parameter decreases as the occupation by Ho atoms increases because of a compression of the M′ site along the trigonal axis. This compression is coupled with a more significant expansion in directions orthogonal to the c axis. This expansion is seen in the larger slope of the line representing the change in the a parameter for $x > 1$.

This interpretation is again supported by results of single-crystal structural studies of the compounds $Sr_6Ho_{0.964}Sc_{1.036}(BO_3)_6$ and $Sr_6Er_{1.4}Sc_{0.6}(BO_3)_6$. In the Ho compound, the Ho:Sc ratio is approximately 1:1, and the larger Ho atom was found to prefer occupation of the larger M site; the occupancy of the M site is 89% Ho and 11% Sc atoms while the occupancy of the M′ site is 93% Sc and 7% Ho atoms. Considering the relative sizes of the Ho and Sc atoms and their distribution over similar octahedral sites, the degree of site preference is rather surprising. This result may be compared to the congruent composition of the garnet GSGG (nominal composition $Gd_3Sc_2Ga_3O_{12}$) where the site occupancies of the 8-fold dodecahedral and 6-fold octahedral sites are $\{Gd_{2.96},Sc_{0.04}\}$ and $\{Sc_{1.86},Ga_{0.14}\}$, respectively.[10] In the Er derivative, the larger Er atom again exhibits a preference for the larger site with occupancies of 91% Er and 9% Sc atoms on the M site and 49% Er and 51% Sc atoms on the smaller M′ site. In this derivative the M′–O distance, 2.144(4) Å, is larger than the corresponding Sc2–O distance, 2.077(2) Å, in the compound $Sr_3Sc(BO_3)_3$. Also, the O2–M′–O2 angle, 83.3(2)°, represents a larger trigonal compression in comparison with the angle O2–Sc2–O2, 85.20(7)°, in the simple Sc derivative, a result that is consistent with the contraction of the c axis for $x > 1$ (Figure 4) and occupation of the M′ site by a larger atom.

The results of substituting larger lanthanides into the structure are partially revealed by the solid-solution series $Sr_6La_xSc_{2-x}(BO_3)_6$. Because of the absence of the phase "$Sr_3La(BO_3)_3$", incomplete solid solubility exists in this series and $x_{max} \approx 0.8$. This result, determined from powder X-ray measurements (Figure 5), is consistent with the stoichiometry found from the single-crystal study of the compound $Sr_6La_{0.84}Sc_{1.16}(BO_3)_6$. We also found that the La atom occupies the 9-coordinate A site. As x increases in the La–Sc series, the Sr atoms likely slip off the A sites and substitute for the Sc atoms on the M sites, being replaced in the process by La atoms on the A sites.

For the nominal stoichiometries $Sr_6LnGa(BO_3)_6$ containing the smaller Ga atom ($r(Ga^{3+}) = 0.76$ Å), STACK derivatives have also been found to exist for the complete lanthanide series. For the Al compounds $Sr_6LnAl(BO_3)_6$ ($r(Al^{3+}) = 0.675$ Å), however, the structure is formed only with those lanthanides up to the size of Sm. From these results, approximate limits on the

(10) Fratello, V. J.; Brandle, C. D.; Valentino, A. J. *J. Cryst. Growth* **1987**, *80*, 26.

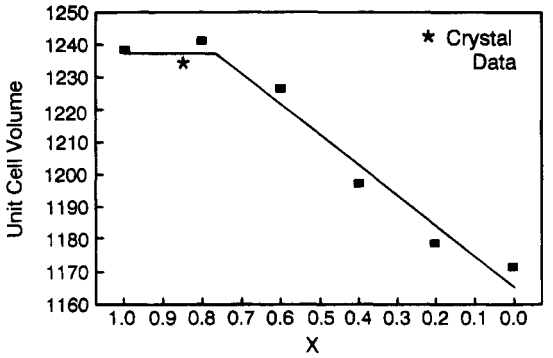

Figure 5. Unit-cell volumes (Å^3) for the solid solution series $Sr_6La_xSc_{2-x}(BO_3)_6$.

structure field of the Sr subclass containing M ≠ M′ can be set forth. The primary constraint appears to be occupation of the M site by an atom that is at least as large as Sc. We speculate that this is achieved with the larger Ln atoms in the Ln−Ga series by cosubstitution of Sr and Ga atoms on the M site in a manner similar to that of the compound $Sr_6La_{0.84}Sc_{1.16}(BO_3)_6$, where Sr and Sc atoms occupy the M site. This cosubstitution does not occur in the Ln−Al series because the Al atom is just too small to occupy the M site. The only other constraint on the formation of this subclass is the upper size of the M′ atom which can not exceed that of a Gd atom.

Because larger lanthanides exhibit a preference for occupation of the large A site, a means is provided for the introduction of smaller *dipositive* cations. Examples of these materials include the nominal formulations $LaSr_5ScZn(BO_3)_6$ (A = La and Sr, M = Sc, and M′ = Zn) and $LaSr_5HoCo(BO_3)_6$ (A = La and Sr, M = Ho, and M′ = Co). From consideration of all the previous results, we anticipate that the small Zn^{2+} (r = 0.88 Å) and Co^{2+} (r = 0.79 Å) ions occupy the M′ sites. By charge compensating in this way, it is likely that any dipositive transition-metal ion that will occupy an octahedral site can be stoichiometrically incorporated into the structure. By substituting two large lanthanides onto the A site it is possible to place dipositive ions on both the M and M′ sites as exemplified by the derivatives $(La_2Sr_4)CaZn(BO_3)_6$ and $(La_2Sr_4)CdCd(BO_3)_6 \equiv LaSr_2Cd(BO_3)_3$. Results on these derivatives are similar to those found for the simpler compounds $A_6MM'(BO_3)_6$, where A = Sr and M and M′ are +3 cations. The compound "$(La_2Sr_4)MgMg(BO_3)_6$" does not exist. The Mg^{2+} ion (r = 0.86 Å) is slightly smaller than the Sc^{3+} ion, so the absence of this compound is consistent with the result that an atom at least as large as Sc must be present at the M site for stabilization and existence of the phase. The presence of $La_2Sr_4CdCd(BO_3)_6$ and nonexistence of "$La_2Sr_4CaCa(BO_3)_6$" is consistent with the series $Sr_6LnLn(BO_3)_6$ where the largest lanthanide incorporated is Gd. The crystal radius of Cd^{2+} (r = 1.09 Å) is intermediate to those of the ions Gd^{3+} and Eu^{3+}, while the radius of Ca^{2+} (r = 1.14 Å) is much larger.

A collection of compounds with M = cation of formal charge +2 and M′ = cation of formal charge +4 has also been prepared. In this family M = Ca, Sr, or Cd and M′ = Zr, Hf, or Sn. Reactions designed to produce STACK derivatives containing Ti^{4+} gave products other than those desired; this result may simply reflect the unreactivity of the reagent TiO_2 that was used in these preparations. The sizes of the ions Zr^{4+} (r = 0.86 Å), Hf^{4+} (r = 0.85 Å), and Sn^{4+} (r = 0.83 Å) indicate they are likely to occupy the M′ site. The distribution of X-ray intensities in the powder patterns is also consistent with this supposition. Existence of the compound $Sr_7Zr(BO_3)_6 \equiv Sr_6SrZr(BO_3)_6$ clearly demonstrates that the Sr atom will fully occupy the M site. Because we have found a limited solubility of Ca on the A site (vide infra), we anticipate that the Ca atom will prefer the larger M site in this subclass.

Before considering the characteristics of the Ba analogues, it is useful to analyze the results of the single-crystal studies in more detail. Interatomic distances for each of the structure refinements are listed in Table 4. For the Sr derivatives, the average A−O and B−O distances are statistically equivalent. The M−O1 and M′−O2 distances associated with the disordered M and M′ sites agree favorably with averages of crystal radii that are determined by weighting the radii according to the site occupancies. For example, the distance 2.477(5) Å for the M−O1 interaction in the compound $Sr_6La_{0.84}Sc_{1.16}(BO_3)_6$ compares to the length 2.49 Å computed for a 6-coordinate site comprised of 0.84 Sr and 0.16 Sc atoms bound by 4-coordinate O atoms. For each derivative, the average A−O distances decrease in the order A−O2 > A−O3 > A−O1. The short average A−O1 distance is consistent with the 4-coordination of atom O1 and the 5-coordination of atoms O2 and O3. While atom O2 binds three Sr atoms, one M′ atom, and one B atom, atom O3 binds four Sr atoms and the B atom. So, the A−O interatomic distances also scale with the distribution of electron density that is expected from a consideration of the relative electronegativities of the coordinating metal atoms. The longer A−O2 interactions are also associated with the shared triangular face of the M′-centered octahedron, where there is a trend of increasing A−O2 lengths with increasing size of the M′ atom. For example, in the Y−Al compound the M′−O2 distance is 1.931(8) Å, and the average A−O2 distance is 2.72(9) Å; in the Er−Sc analog the M′−O2 distance is 2.144(4) Å, and the average A−O2 distance is 2.78(2) Å. Additional indications that the La atom resides on the A site in the La−Sc derivative are seen from the shortened A−O1 distances ($r(La^{3+})$ = 1.36 Å and $r(Sr^{2+})$ = 1.45 Å) and a general lengthening of the A−O3 distances.

Interatomic angles are listed in Table 5. A rather notable consistency is observed in these data, as corresponding interatomic angles deviate by no more than 3° among the various structures. A curious result is observed in the La−Sc derivative—the regular M environment with the O1−M−O1 angle of 91.9(2)° most closely approaches orthogonality among these derivatives, while the M′ environment is characterized by the largest trigonal compression (O2−M′−O2 = 82.4(2)°.) Adjacent MO_6 and $M'O_6$ octahedra along the C_3 chain axis are rotated by approximately 30°, one relative to the other. The largest deviation, 2.7°, from this angle is observed in the Y−Al derivative.

The structure fields of the Ba derivatives are much more restricted than those of the Sr analogues. The compound $Ba_3In(BO_3)_3$ is the only Ba derivative containing M = M′. We have prepared several examples with M and M′ being different cations of formal charge +3 (cf. Table 3); no Al or Ga derivatives, however, could be crystallized. In the series $Ba_6LnIn(BO_3)_6$, incorporation of each lanthanide produces the STACK structure.

Table 4. Interatomic Distances (Å) for STACK Derivatives

	$Sr_6Y_{1.07}Al_{0.93}(BO_3)_6$	$Sr_6Er_{1.40}Sc_{0.60}(BO_3)_6$	$Sr_6Ho_{0.964}Sc_{1.036}(BO_3)$	$Sr_6La_{0.84}Sc_{1.16}(BO_3)_6$	$Ba_6Gd_{1.28}Sc_{0.72}(BO_3)_6$
A–O1	2.523(8)	2.530(4)	2.520(4)	2.473(5)	2.657(7)
–O1	2.643(8)	2.707(5)	2.683(4)	2.589(5)	2.799(7)
–O2	2.632(8)	2.768(4)	2.728(4)	2.709(6)	2.872(6)
–O2	2.810(8)	2.798(4)	2.799(4)	2.858(6)	2.975(6)
–O2	2.706(8)	2.763(5)	2.752(4)	2.723(6)	2.883(6)
–O3	2.886(9)	3.033(5)	2.983(5)	3.069(6)	3.110(6)
–O3	2.578(8)	2.495(5)	2.529(4)	2.512(5)	2.700(6)
–O3	2.561(8)	2.569(4)	2.569(5)	2.589(6)	2.746(6)
–O3	2.727(9)	2.761(5)	2.763(4)	2.769(6)	2.902(6)
A–O (av)	2.67(12)	2.71(16)	2.70(15)	2.70(18)	2.85(14)
M–O1	2.250(8)	2.291(4)	2.295(4)	2.477(5)	2.423(7)
M′–O2	1.931(8)	2.144(4)	2.090(4)	2.125(5)	2.162(5)
B–O1	1.37(1)	1.386(7)	1.393(7)	1.361(9)	1.40(1)
–O2	1.41(1)	1.386(7)	1.390(7)	1.390(9)	1.374(9)
–O3	1.37(1)	1.352(8)	1.353(7)	1.359(9)	1.36(1)
B–O (av)	1.38(2)	1.37(2)	1.38(2)	1.37(2)	1.38(2)

Table 5. Interatomic Angles (deg) for STACK Derivatives

	$Sr_6Y_{1.07}Al_{0.93}(BO_3)_6$	$Sr_6Er_{1.40}Sc_{0.60}(BO_3)_6$	$Sr_6Ho_{0.964}Sc_{1.036}(BO_3)$	$Sr_6La_{0.84}Sc_{1.16}(BO_3)_6$	$Ba_6Gd_{1.28}Sc_{0.72}(BO_3)_6$
O1–A–O1	155.5(3)	158.6(2)	157.4(1)	158.7(2)	159.7(2)
O1–A–O2	96.6(2)	90.7(1)	91.9(1)	88.7(2)	93.5(2)
	75.3(2)	77.3(1)	77.2(1)	80.4(2)	74.6(2)
	105.7(2)	109.4(1)	108.9(1)	109.2(2)	105.3(2)
O1–A–O3	51.9(2)	50.0(1)	50.7(1)	49.4(1)	48.2(2)
	85.2(3)	87.9(1)	87.1(1)	89.7(2)	86.0(2)
	72.6(3)	72.5(1)	72.4(1)	74.9(1)	73.9(2)
	70.4(2)	70.7(1)	70.4(1)	70.4(2)	71.9(2)
O2–A–O2	63.3(3)	62.1(6)	61.2(1)	62.1(2)	66.4(2)
	58.2(3)	61.7(2)	60.3(1)	60.2(2)	59.5(2)
O2–A–O3	75.1(2)	70.6(1)	71.4(1)	78.6(2)	77.7(2)
	78.0(2)	78.0(1)	78.1(1)	78.2(2)	80.3(2)
	74.4(2)	70.7(1)	71.8(1)	73.0(2)	73.6(2)
O3–A–O3	83.26(9)	85.0(2)	85.3(1)	83.8(2)	84.43(6)
	86.9(3)	86.2(1)	86.0(1)	86.0(1)	87.1(2)
O1–M–O1	93.1(3)	92.5(2)	92.3(1)	91.9(2)	93.4(2)
O2–M′–O2	84.5(3)	83.3(2)	83.7(2)	82.4(2)	84.5(2)
O1–B–O2	119(1)	117.3(5)	117.8(5)	118.1(6)	117.9(7)
O1–B–O3	121(1)	122.2(5)	121.2(5)	122.0(5)	120.2(7)
O2–B–O3	120(1)	120.5(5)	121.0(5)	119.9(6)	121.9(7)

In the series $Ba_6LnFe(BO_3)_6$ only those compounds containing Ln = Sm, Eu, Gd, Tb, Dy, Ho, Y, and Er were found to form the structure, while in the series $Ba_6LnSc(BO_3)_6$ only those compounds containing Ln = La, Pr, Nd, Sm, Eu, Gd, Tb, and Dy could be formed. In the Fe and Sc series a sufficient radius ratio between these atoms and the Ln atoms must be present for the STACK structure to form. For the Fe series the minimum ratio (Ln/Fe) occurs at Ln = Er, and for the Sc series it occurs at Ln = Dy. These limits are dictated by the formation of the layered phases of the $Ba_3Sc(BO_3)_3$ structure type that was discussed in the previous report of this series. For the Fe derivatives, layered-type phases form when the radius of the Ln atom is smaller than that of Er. We have not determined whether these phases are simple $Ba_3Ln(BO_3)_3$ compounds or more complex examples involving Fe substitution on the Ln site. For the Sc compounds, solid solutions $Ba_3(Ln,Sc)(BO_3)_3$ form in the layered structure type when Ln is smaller than Dy.

Although the structures of STACK and the layered-type Ba phases are rather complex and distinctive, the energetic difference between them can apparently be quite small. An example of this behavior is given by the solid-solution series $Ba_6Sc_{2-x}Dy_x(BO_3)_6$. This series represents equilibria between the two end members $Ba_3Sc(BO_3)_3$ and $Ba_3Dy(BO_3)_3$, both examples of the layered-type structure. As seen in Figure 6, a complete solid solution exists in this series with retention of the layered structure, except near the stoichiometry $Ba_6DyDy(BO_3)_6$ where a considerable expansion of the unit cell is observed, and the STACK structure forms.

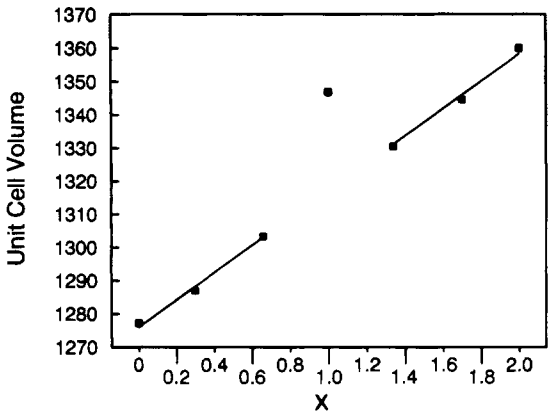

Figure 6. Unit-cell volumes (Å^3) for the series $Ba_6Sc_{2-x}Dy_x(BO_3)_6$.

We also probed the relationship between the STACK and layered-type structures by examining the solid-solution series $Ba_{3-x}Sr_xSc(BO_3)_3$. In this series, the compound $Ba_3Sc(BO_3)_3$ forms the layered structure, and $Sr_3Sc(BO_3)_3$ is a STACK derivative. As seen in Figure 7, a steady decrease in unit-cell volume in the range $0 < x < 2.25$ indicates an extensive range of solubility of Sr atoms in the Ba layered structure. (No attempt was

(11) Superstructures have been identified for intermediate compositions by single-crystal X-ray methods. Huang, J., Keszler, D., unpublished results.

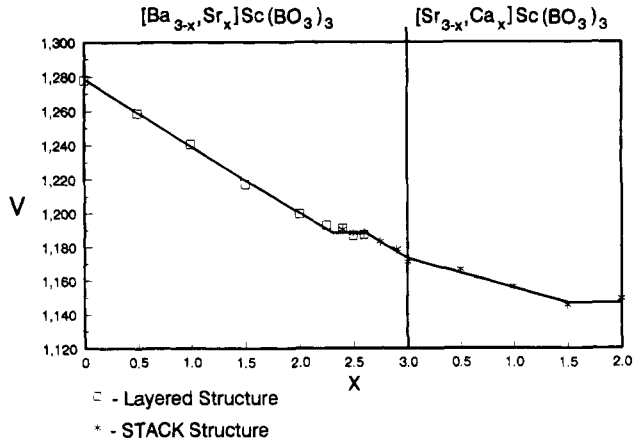

Figure 7. Unit-cell volumes (Å^3) for the series $Ba_{3-x}Sr_xSc(BO_3)_3$ and $Sr_{3-x}Ca_xSc(BO_3)_3$.

made here to identify in the powder X-ray patterns superstructure ordering of the Sr and Ba atoms.)[11] The zero slope in the range $2.25 < x < 2.6$ defines a region of immiscibility, i.e., the layered-type and STACK structures are present in equilibrium mixtures. In the range $2.6 < x < 3$, only the STACK structure is observed with a steady decrease in unit-cell volume with increasing x; this region represents the solid solubility of Ba^{2+} in the STACK derivative. These results were extended with examination of the series $Sr_{3-x}Ca_xSc(BO_3)_3$. As seen from Figure 7, the level of Ca incorporation is limited to $x_{max} = 1.5$. The Ca atom is too small to completely occupy the large 9-coordinate A site where, for this derivative, the size of the site is largely determined by the dimensions of the one-dimensional Sc borate chains. This result appears tp be consistent with the structure of the simpler compound $Ca_3(BO_3)_2$ where the Ca atom is surrounded by only eight O atoms.[12,13] To the extent that the level of Ca solubility is determined by the sizes of the M and M′ atoms and the dimensions of the chains, we expect the greatest Ca solubility at the A site to be realized with M = Sc and M′ = Al, where the unit-cell volume is minimized.

Existence of the compounds $Ba_6LaIn(BO_3)_6$ and $Ba_6LaSc(BO_3)_6$ raises questions as to the site occupancies by the larger lanthanides. Because of their similar atomic scattering factors (Ba vs La), we cannot readily deduce this distribution from a visual examination of the peak intensities in the powder X-ray diffraction patterns. Such information, however, could be deduced from the interatomic-distance results of a single-crystal X-ray study. As for the Sr derivatives, such a study would also reveal the extent of disorder and nonstoichiometry in these phases.

Attempts to prepare Ba derivatives with M = +2 cation and M′ = +4 cation typically resulted in products that were not single phase. Compounds containing M = Sr, however, were found to be stable, highly crystalline compounds (cf. Table 3). The existence of $Ba_6SrZr(BO_3)_6$ together with that of $Sr_6SrZr(BO_3)_6$ indicates that complete solubility may exist for the series $Sr_{6-x}Ba_xSrZr(BO_3)_6$. Likewise, similar solubility characteristics may be expected for those Ba and Sr derivatives containing the same M and M′ atoms.

Conclusions

The borates of composition $A_6MM'(BO_3)_6$ represent a broad new class of oxide. By utilizing appropriate charge-compensation techniques, nearly all +2, +3, and +4 ions of the elements in the periodic table can be incorporated into the structure. From detailed powder and single-crystal X-ray results, it appears likely that extensive solid-solution behavior and perhaps considerable nonstoichiometry will be a common trait for many of the nominal compositions listed in Table 3. Analysis of the metrical details from the single-crystal studies also reveals little variation in nearest-neighbor interatomic angles. This feature, coupled with the centrosymmetric S_6 symmetry of the M and M′ sites, indicates that physical properties, e.g., luminescent characteristics of dopant ions and magnetic interactions, will be primarily controlled by interatomic distances, the electronic nature of the A, M, and M′ atoms, stoichiometry, and disorder, rather than any significant structure distortions. Some of these considerations will be addressed in forthcoming contributions.

Acknowledgment. Acknowledgment is made to the National Science Foundation and the donors of the Petroleum Research Fund, administered by the American Chemical Society, for support of this research. Work on the Sc derivatives was supported through Lawrence Livermore National Laboratory by the Department of Energy (Contract W-7405-ENG-48). D.A.K. expresses gratitude to the Alfred P. Sloan Foundation for a fellowship, and K.I.S. acknowledges Pacific Northwest Laboratories for a DOE graduate fellowship.

Supplementary Material Available: Listings of complete crystal data and anisotropic displacement coefficients (4 pages); list of observed and calculated structure factors (30 pages). Ordering information is given on any current masthead page.

(12) Vegas, A.; Cano, F. H.; Garcia-Blanco, S. *Acta Crystallogr., Sect. B* **1975**, *31*, 1416.
(13) Schuckmann, W. *Neues Jahrb. Mineral., Monatsh.* **1969**, *3*, 142.